*sustainability*

MDPI

*Article*

# Unraveling the Effect of Kraft and Organosolv Processes on the Physicochemical Properties and Thermal Stability of Cellulose and Its Microcrystals Produced from Eucalyptus Globulus

**Wissam Bessa [1,2,*], Djalal Trache [2,*], Ahmed Fouzi Tarchoun [1,3], Amir Abdelaziz [2], Mohd Hazwan Hussin [4] and Nicolas Brosse [5]**

1 Ecole Supérieure du Matériel ESM, BP 188, Beau-Lieu, Algiers 16004, Algeria
2 Energetic Materials Laboratory, Ecole Militaire Polytechnique, BP 17, Bordj El-Bahri, Algiers 16046, Algeria
3 Energetic Propulsion Laboratory, Ecole Militaire Polytechnique, BP 17, Bordj El-Bahri, Algiers 16046, Algeria
4 Materials Technology Research Group (MaTReC), School of Chemical Sciences, Universiti Sains Malaysia, Minden 11800, Penang, Malaysia
5 Laboratoire d'Etude et de Recherche sur le MAtériau Bois (LERMAB), Faculté des Sciences et Techniques, Université de Lorraine, Bld. des Aiguillettes, 54500 Vandœuvre-lès-Nancy, France
* Correspondence: wsambes@gmail.com (W.B.); djalaltrache@gmail.com (D.T.)

**Abstract:** Eucalyptus Globulus (EG) is a virtually untapped forest source that belongs to the hardwood family. The objective of this research is to understand the effect of two different isolation techniques, i.e., kraft and organosolv procedures, followed by either acidified sodium chlorite or alkaline hydrogen peroxide treatment on the properties of cellulose and microcrystalline cellulose (MCC) derived from EG. The MCC samples were successfully prepared from cellulose via acid hydrolysis. A comparative study was carried out on the extracted cellulose fibers and MCC samples through deep characterizations of lignocellulosic content, functional groups, crystallinity, thermal properties, and surface morphology. The detailed analyses exhibited that the prepared MCC samples using various approaches are similar to those of commercial MCC. It is revealed that the organosolv treatment followed by acidic bleaching provides the purest MCC with good thermal features, where the obtained cellulose has a glucose content of more than 97% and a degradation temperature of around 343 °C. The present work provides new insight into the effect of various extraction procedures on EG-MCC; these procedures are expected to be used in different industrial applications such as in biorefinery, dietary food, packaging, films, or reinforcement of polymer matrices.

**Keywords:** eucalyptus globulus; cellulose; microcrystalline cellulose; organosolv; kraft; characterization



**Citation:** Bessa, W.; Trache, D.; Tarchoun, A.F.; Abdelaziz, A.; Hussin, M.H.; Brosse, N. Unraveling the Effect of Kraft and Organosolv Processes on the Physicochemical Properties and Thermal Stability of Cellulose and Its Microcrystals Produced from Eucalyptus Globulus. *Sustainability* **2023**, *15*, 3384. https://doi.org/10.3390/su15043384

Academic Editors: Jianxin Jiang, Jun Hu, Hailong Yu and Mariateresa Lettieri

Received: 11 December 2022
Revised: 8 February 2023
Accepted: 9 February 2023
Published: 13 February 2023



## 1. Introduction

In recent decades, lignocellulosic biomass has become a massively attention-grabbing matter for miscellaneous applications beyond paper production. The huge interest in achieving greener societies and countries and the increasing support of ecosystems and ecological safety has prompted scientists and industry to turn to renewable solid and carbon-neutral natural-based materials including natural lignocellulosic fiber-based materials [1]. Cellulose is the most abundant polymer on Earth; this compound was identified in 1839 by the French chemist Anselme Payen, who found that plant cells are constituted of fibrous substances built from uniform carbohydrates. This matter was later named by the French Science Academy "cellulose" which means "sugar from cells" [2]. A panoply of cellulose extraction techniques exists, developed over several years, especially in terms of delignification and bleaching, and many pieces of research have been published about this subject [3–8]. This subject has continued to attract more and more research worldwide toward an understanding of the different aspects involved to produce effective, sustainable, and high-value products.

In fact, lignocellulosic biomass is inherently recalcitrant and hard to dissociate because of the interconnection of cellulose in the hemicellulose–lignin matrix [9]. Thus, it is crucial to explore diverse treatment techniques and assess the pros and cons of each in order to identify a suitable method for the intended application. Furthermore, the amplified awareness of the negative ecological impacts of the longstanding bleaching techniques have led to the use of fewer pollutants and the implementation of new eco-friendly approaches, including the fractionation of lignocellulosic biomass to separate beneficial fractions. Indeed, it is essential to explore new sources of cellulose using more sustainable and effective extraction techniques to ensure a commitment to the environment. According to this concept, it would be interesting to harness extraction techniques such as kraft and organosolv, which are known for their ability to fractionate biomass in order to separate beneficial fractions in such a way that the recovered lignin and cellulose could be further used in various applications, such as biofuel, biorefinery [10], and the paper industry [11], which present an interesting factor for the development of sustainable materials.

Kleinert and Tayenthal developed the organosolv pretreatment, also called solvent cooking, in 1931 for pulp delignification by extracting lignin using aqueous solutions or organic solvents [10,12]. This treatment is an economically promising method due to the ability to easily recover the involved solvents [13]. Indeed, it provides an effective fractionation of lignocellulosic feedstock through an organic solvent, producing a cellulose-rich pulp with minor degradation, organosolv lignin fraction, hemicellulose, and oligosaccharides as syrup, with no structure changes, ensuring the high significance of the byproducts [14–16]. The process breaks down the lignin and hemicellulose bonds; then, it hydrolyzes the internal lignin bonds and ether and the 4-O-methylglucuronic acid ester bonds among hemicellulose and lignin, in addition to the hemicellulose glycosidic linkages, leading to the degradation of aromatic rings [17]. From a technical and operational point of view, organosolv treatment has revealed significant commercial practicability as a factual substitute for traditional technologies [18], yet it is still not commonly adopted to date [19].

Kraft pulping, another treatment approach that enables obtaining separate fractions of cellulose and lignin, was first introduced in 1870 and 1871. Its industrial application was made possible in 1879 by Dahl [20]. Kraft pulping technology is nowadays predominant in the world with a large knowledge base from the laboratory scale to industrial uses. It is the largest alkaline process that uses a combination of sodium hydroxide and sodium sulfide for lignin removal from lignocellulosic materials [7]. Kraft pulping produces high-strength pulp and enables the recovery of chemicals and power which make it an efficient and economical process [21]. During this process, the reagents cause the cleavage of β-aryl-ether linkages in lignin [22], leading to instantaneous delignification of wood to cellulose, hence avoiding carbohydrate damage.

Nevertheless, when these processes are utilized for cellulose isolation, further post-treatments are required for bleaching and/or taking out chromophores present in the fibers [23]. Indeed, it is reported that this treatment combination approach results in a separation of cellulose, lignin, and hemicellulose [10,24] with high purity, which is a sought-after target in many applications.

The most adopted ways to recover pure cellulosic fibers are the alkali and acid-chlorite treatments, which ensure the effective removal of residual lignin and hemicellulose from the biomass. Despite recent delignification methods that have been developed such as ionic liquids and deep eutectic solvents, the acidified sodium chlorite method remains the most commonly used process for bleaching the lignocellulosic biomass and hence destroying the complex hierarchical microstructure and its recalcitrance to produce high value-added cellulosic products [6]. The alkaline peroxide method is another prominent approach that offers many advantages such as low cost, safety, and stable end-products [25]. It is reported that this treatment can promote the exclusion of the greater part of amorphous compounds such as lignin, ashes, pectin, and hemicellulose [26].

Eucalyptus is a fast-growing hardwood that is mainly exploited for pulp, paper, and solid wood production. It is characterized by high cellulose content and low lignin and

extractives amounts [27]. Among the various eucalyptus species, Eucalyptus Globulus (EG) has many advantages such as high wood density and excellent fiber quality [28]. Therefore, to fully benefit from this natural resource, understanding the properties of the derived products such as α-cellulose and microcrystalline cellulose (MCC), also known as cellulose microcrystals, through different isolation processes is crucial to select the most effective one for an intended application. It is worth mentioning that MCC, which displays outstanding properties such as renewability, high mechanical features, lightness, stiffness, water insolubility, fibrous nature, good thermal stability, and high crystallinity, is currently employed in various industries ranging from pharmaceutics to biocomposites. Its market size is expected to reach $1241.4 million in 2023 owing to the increasing demand in current and emerging applications [29].

This paper aims to investigate and compare combinations of isolation procedures in order to obtain highly pure cellulose from Eucalyptus Globulus. For that, two delignification techniques, kraft and organosolv, were undertaken followed by a bleaching process using either acidified sodium chlorite or alkaline peroxide treatments. The obtained samples were further converted to cellulose using a sodium hydroxide solution. The isolated α-cellulose is then employed to produce MCC via acid hydrolysis. To the best of our knowledge, the chosen procedures have never been compared before for cellulose and MCC extraction from EG, and thus represent a benefit in the field of exploring sustainable and bio-sourced materials. The obtained products were characterized using Fourier-transform infrared spectroscopy (FTIR), $^{13}C$ nuclear magnetic resonance spectroscopy (NMR), gel permeation chromatography (GPC), scanning electron microscopy (SEM), cellulose purity determination, and thermal analysis by thermogravimetric analysis (TGA) and differential scanning calorimetry (DSC) to highlight the changes occurring on the obtained cellulose and MCC samples and identify the process that produces the MCC with the best quality.

## 2. Experimental Section

### *2.1. Materials and Methods*

All chemicals employed during biomass treatments and MCC preparation are of analytical grade and were used without prior purification.

#### 2.1.1. Preparation of the Biomass Samples

This paper aims to prepare α-cellulose and microcrystalline cellulose from Eucalyptus and investigate the efficiency of the used processes. Dried wood chips of EG were ground to less than 2 mm in diameter and oven dried at 40 °C for 24 h. To eliminate the organic extractives from the natural fibers, a Soxhlet extraction was performed using a solvent mixture of toluene/ethanol (2:1, *v*/*v*) for 48 h.

#### 2.1.2. Cellulose Extraction

The obtained wood fibers were then subjected to delignification using either the kraft or ethanol–organosolv treatment in a Parr pressure reactor (0.6 L) with a Parr 4842 temperature controller (Parr Instrument Company, Moline, IL, USA). After that, the recovered solid samples were treated either by acidified sodium chlorite or alkaline peroxide delignification. The resulting hollocellulose samples were converted to α-cellulose using a sodium hydroxide solution. The procedure details are illustrated in Scheme 1.

#### 2.1.3. MCC Preparation

The obtained bleached cellulose samples were transformed to MCC by hydrolysis using hydrochloric acid 2.5 N for 30 min at 105 °C, washed with water and sodium hydroxide solution, and finally dried to obtain the respective MCC samples. Depending on the adopted method, the samples were named as presented in Table 1.

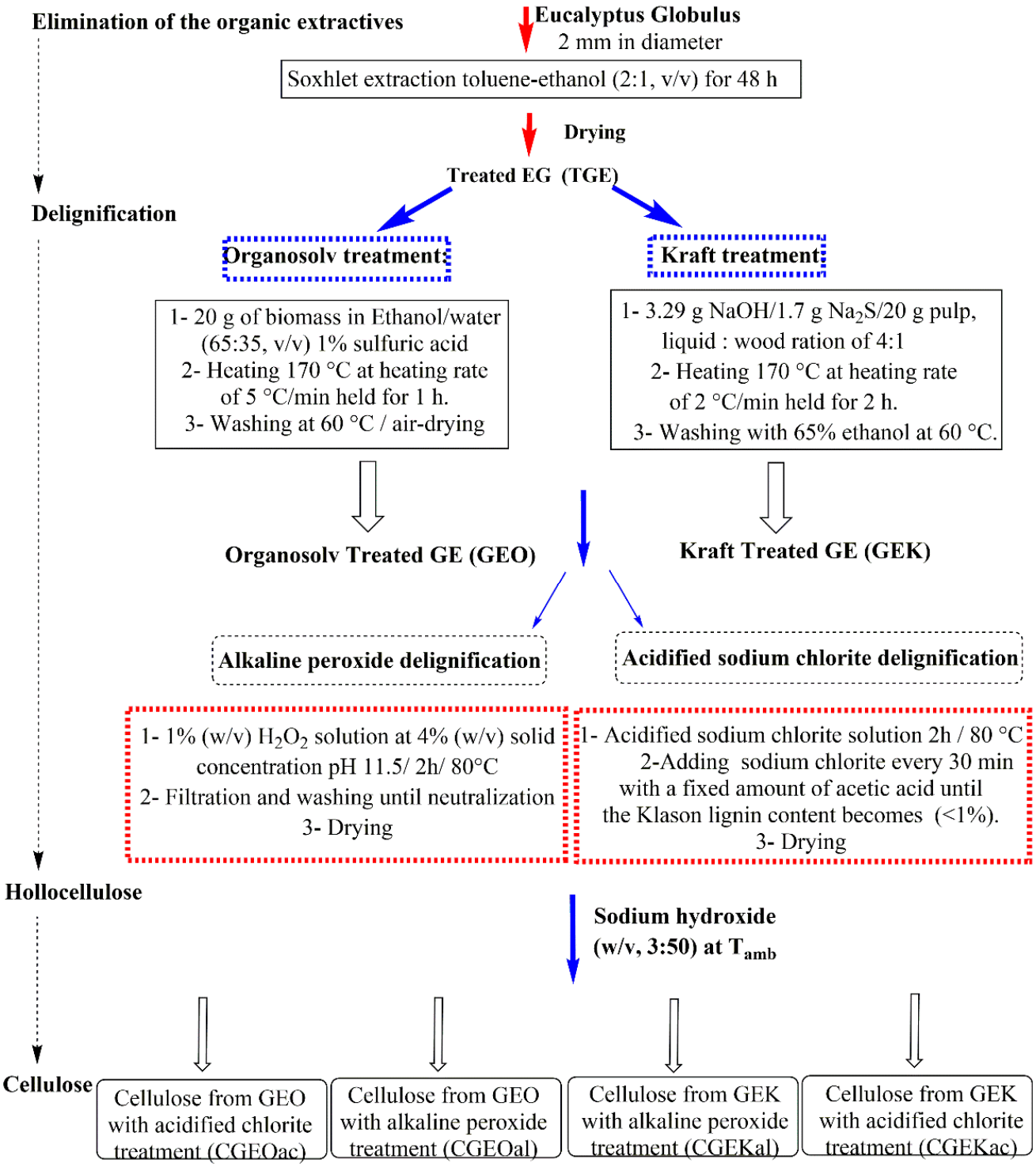


**Scheme 1.** Detailed extraction procedures of the α-cellulose by kraft and organosolv techniques, followed by either acidified sodium chlorite or alkaline hydrogen peroxide treatment.

**Table 1.** Cellulose and MCC sample designations according to the employed process.

| Sample Name | Employed Procedure |
|---|---|
| CGEOac | Cellulose from EG by organosolv and acidified sodium chlorite solution |
| CGEOal | Cellulose from EG by organosolv and alkaline peroxide solution |
| CGEKac | Cellulose from EG by kraft and acidified sodium chlorite solution |
| CGEKal | Cellulose from EG by kraft and alkaline peroxide solution |
| MCCGEOac | MCC from EG by organosolv and acidified sodium chlorite solution |
| MCCGEOal | MCC from EG by organosolv and alkaline peroxide solution |
| MCCGEKac | MCC from EG by kraft and acidified sodium chlorite solution |
| MCCGEKal | MCC from EG by kraft and alkaline peroxide solution |

### *2.2. Characterization*

#### 2.2.1. Fourier-Transform Infrared Spectroscopy Analysis

A Shimadzu 8400S spectrometer was used for FTIR analyses. The samples were embedded in KBr pellets and analyzed in transmittance mode within a wavenumber range from 4000 to 600 $cm^{-1}$ at a resolution of 4 $cm^{-1}$.

##### 2.2.1.1. $^{13}C$ Nuclear Magnetic Resonance Spectroscopy

A Burker Avance-300 spectrometer was employed to perform the solid-state NMR experiments using a 4 mm cross-polarization magic angle spinning (CP/MAS) at a working frequency of 76.46 MHz. Samples were pressed into cylindrical zirconia rotors and spun at a magic angle at 7 kHz. The spectra were recorded as the sum of 4000 scans and calibrated using the methane carbon atoms of adamantane as an external standard ($\delta$ = 29.47 ppm). Data were processed by XWinNMR software with a line broadening of 10 Hz.

#### 2.2.2. Scanning Electron Microscopy

A Hitachi S-4800 scanning electron microscope was used to record sample morphologies. Carbon coating was ensured by the arc discharge method. A secondary electron mode was used for the morphology scan.

#### 2.2.3. Cellulose Purity by Sugar Analysis

The hydrolysis method was employed to determine the chemical composition of the different samples. Anion exchange chromatography with a pulsed amperometric detector (HPAEC-PAD), Dionex ICS-3000 system, was used to quantify monosaccharide contents. The complete followed method is reported in our previous work [30].

#### 2.2.4. Gel Permeation Chromatography

Cellulosic samples were derivatized to cellulose tricarbanilate (CTC) using phenyl isocyanate. The tricarbanilation process was achieved following the procedure reported elsewhere [30]. The derivatives were dissolved in tetrahydrofuran (THF), filtered through a 0.45 µm Teflon membrane, and placed in a 2 mL auto-sampler vial preceding the GPC analysis. In order to avoid random error, four analyses were implemented. The measurement error is thus the standard deviation calculated from four measurements. The number-average molecular weight (Mn) and weight-average molecular weight (Mw) were determined using the Dionex Ultimate-3000 HPLC system with a UV detector with THF as the eluent. Analyses were held at 30 °C at a flow rate of 1 mL/min. The calibration curves were built using standard polystyrene samples and data collection and analysis were ensured by Chromeleon software version 6.8 (Dionex Corp., Sunnyvale, CA, USA). The cellulose derivatives were identified at a wavelength of 235 nm.

2.2.5. Thermal Analysis

A Setaram Setsys 12 differential scanning calorimetry–thermogravimetric analyzer (DSC–TGA) was employed for simultaneous thermal analysis. Samples of about 6 mg were analyzed from 50 °C to 700 °C under a nitrogen atmosphere at 10 °C/min.

## 3. Results and Discussion

### *3.1. Chemical Composition of the Samples by HPAEC-PAD Analysis*

The chemical composition of the prepared samples was analyzed by HPAEC-PAD and summarized in Table 2. The aim was the determination of sample purity and quantification of the composition changes occurring during treatments.

**Table 2.** Chemical composition of the prepared samples.

| | **E. Globulus (g/100 g)** | **GEO (g/100 g)** | **GEK (g/100 g)** | **CGEOac (g/100 g)** | **CGEOal (g/100 g)** | **CGEKac (g/100 g)** | **CGEKal (g/100 g)** |
|---|---|---|---|---|---|---|---|
| Glucose | 44.1 ± 0.5 | 84.4 ± 0.4 | 85.9 ± 0.3 | 97.3 ± 0.2 | 96.4 ± 0.1 | 97.9 ± 0.3 | 97.3 ± 0.4 |
| Xylose | 16.4 ± 0.4 | 7.5 ± 0.3 | 10.6 ± 0.5 | 0.97 ± 0.07 | 2.50 ± 0.08 | 0.78 ± 0.05 | 1.10 ± 0.1 |
| Arabinose | 0.41 ± 0.05 | 0.27 ± 0.04 | 0.08 ± 0.02 | 0.04 ± 0.01 | Tr | 0.06 ± 0.01 | Tr |
| Galacturonic acid | 0.45 ± 0.01 | 0.04 ± 0.01 | 0.02 ± 0.01 | 0.44 ± 0.06 | Tr | 0.51 ± 0.08 | 0.47 ± 0.08 |
| Glucuronic acid | 0.62 ± 0.03 | 0.03 ± 0.01 | 0.03 ± 0.01 | Tr | Tr | Tr | Tr |
| Galactose | 1.70 ± 0.07 | 0.42 ± 0.03 | 0.50 ± 0.06 | 0.41 ± 0.05 | 0.46 ± 0.06 | Tr | Tr |
| Klason lignin | 28.6 ± 0.5 | 8.6 ± 0.4 | 2.9 ± 0.7 | Tr | Tr | Tr | Tr |
| Soluble lignin | 1.75 ± 0.47 | 0.42 ± 0.07 | 0.30 ± 0.04 | 0.89 ± 0.04 | 0.93 ± 0.05 | 0.77 ± 0.02 | 0.83 ± 0.07 |
| Extractives | 5.5 ± 0.6 | / | / | / | / | / | / |
| Ashes | 0.32 ± 0.02 | / | / | / | / | / | / |

Tr: traces.

Comparing the composition of native EG with EGO and EGK revealed the efficiency of the delignification processes toward lignin and even hemicellulose elimination. Indeed, Klason and soluble lignin amounts clearly decreased. Furthermore, the contents of xylose, arabinose, galacturonic acid, and glucuronic acid, the principal constituents of hemicellulose [31], were reduced after both treatments. With a minor difference, it seems that the organosolv treatment is less proficient than the kraft treatment toward delignification, especially in Klason lignin elimination. This dissimilarity may be attributed to the harsh hydrolysis conditions and the high selectivity of the Kraft process [32].

From Table 2, it can be seen that the selected acidified chlorite and alkaline peroxide delignification techniques ensured an effective elimination of residual hemicellulose and lignin with an identical affinity in both biomasses. All the cellulosic samples are principally composed of glucose > 96%, suggesting the high cellulose content after the delignification and hemicellulose removal processes. In turn, it is clear that the Klason and soluble lignin content is very low <1%, demonstrating that the employed approaches are selective toward lignin and hemicellulose. The obtained results are in agreement with those obtained for alpha-cellulose extracted from EG using sodium chlorite delignification followed by sodium hydroxide [28].

### *3.2. Chemical Structure of the Samples with Infrared Spectroscopy*

FTIR spectra of all studied samples are presented in Figure 1 with a hint of the main bonds.

The similarity is eminent for all samples with no appearance or disappearance of any peaks. An increase in polysaccharide group intensity within the 1300–900 $cm^{-1}$ range and hydroxide groups stretching vibration around 3400 $cm^{-1}$ is perceived when comparing MCC samples with cellulose samples, which reflect the greatly exposed cellulose domains as a result of acid hydrolysis [33].

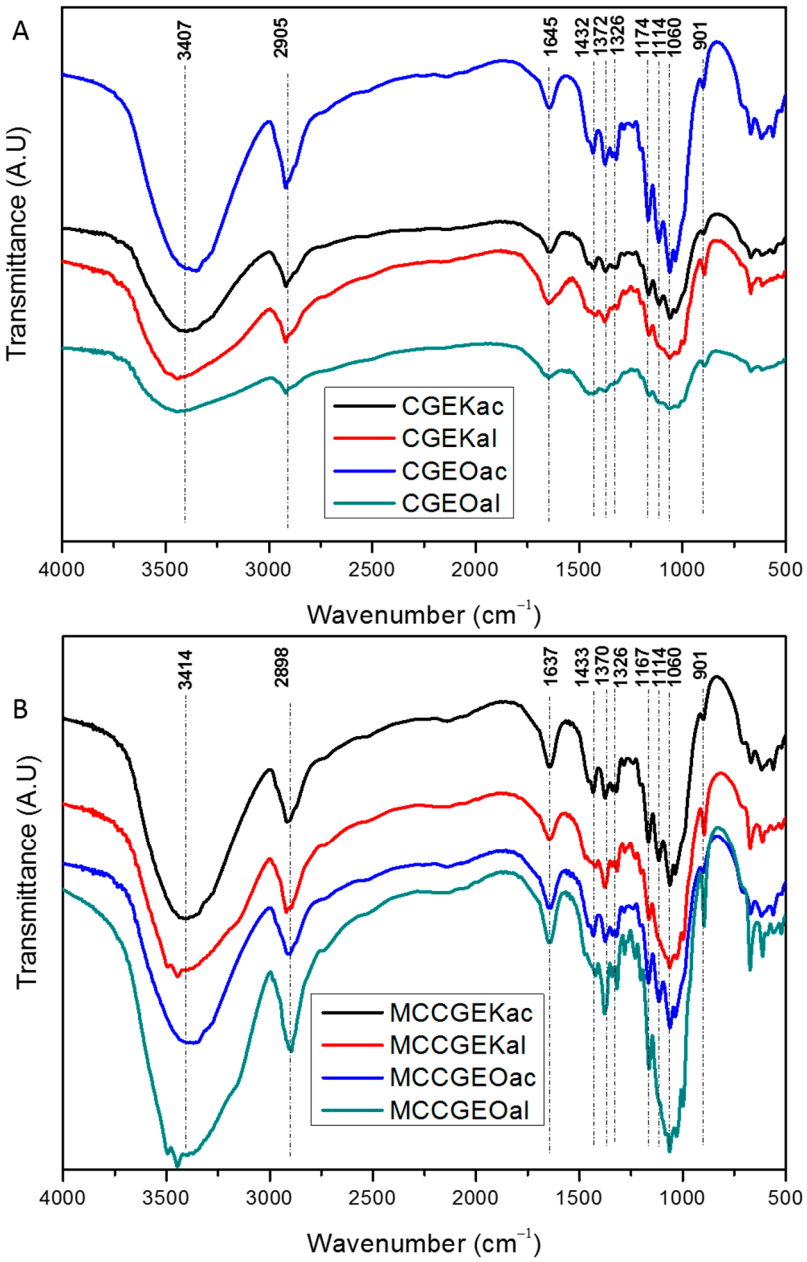


**Figure 1.** FTIR spectra of (**A**) all prepared α-cellulose and (**B**) MCC samples using kraft and organosolv procedures followed by either acidified sodium chlorite or alkaline hydrogen peroxide treatment.

All spectra represent the characteristic peaks of cellulose [34], proving that the cellulose structure through all used treatments is maintained. The band at 2900 cm$^{-1}$ refers to the aliphatic saturated –$CH_2$ stretching vibration, which means that no α-cellulose degradation occurred [6]. The absorbed water peak observed at 1643 cm$^{-1}$ is related to the strong moisture–cellulose interaction. The total removal of lignin is confirmed by the nonappearance of its characteristic peaks at 1512 cm$^{-1}$ and 1250 cm$^{-1}$ assigned to C=C aromatic vibration and C=O, respectively [35]. Similarly, the hemicellulose characteristic peak around 1730 cm$^{-1}$ is imperceptible, which confirms once again its elimination [36].

All MCC and acidified sodium chlorite cellulose samples show the presence of a $CH_2$ symmetric stretching band at around 1430 cm$^{-1}$. This band is known as the crystallinity band, reflecting the high crystallinity degree of the samples, and thus the removal of amorphous regions [37]. The C-H and C-O of the polysaccharide ring stretching vibrations appeared at 1370 cm$^{-1}$, while the $CH_2$ wagging vibrations are seen at around 1325 cm$^{-1}$.

The C-O-C stretching of the β-1,4-glycosidic ring linkages between the cellulose D-glycose units is observed at 1167 $cm^{-1}$, whereas that of the pyranose ring of the cellulose stretching vibration is exhibited at 1110 $cm^{-1}$. The cellulose β-glucosides C-H rock vibration is noted at around 900 $cm^{-1}$.

From the above discussion, it can be concluded that the selected cellulose extraction process guaranteed the protection of the cellulose structure with high effectiveness toward the removal of non-cellulosic substances as established by the chemical composition examination.

### *3.3. NMR Spectroscopy*

In order to provide more information about the samples' structures, NMR analyses were carried out and the obtained spectra are shown in Figure 2. All signals elucidate the recognized cellulose characteristic carbon resonances [38], where each peak has been assigned and displayed on the spectra. The resonance lines of carbons C1, C4, and C6 appeared, respectively, at around 105 ppm, 89 ppm, and 65 ppm. The cluster of overlapped resonances appearing around 75 ppm is attributed to C2, C3, and C5 carbons. Those resonances cannot be, in most cases, assigned individually in solid-state NMR [39]. According to the obtained NMR results, the chosen treatments present good preservation of cellulose with an elimination of the lignin and hemicellulose, as revealed by the complete absence of their characteristic peaks at 20.8 ppm and 172 ppm for hemicellulose and around 154 ppm and 56.5 ppm for lignin [40].

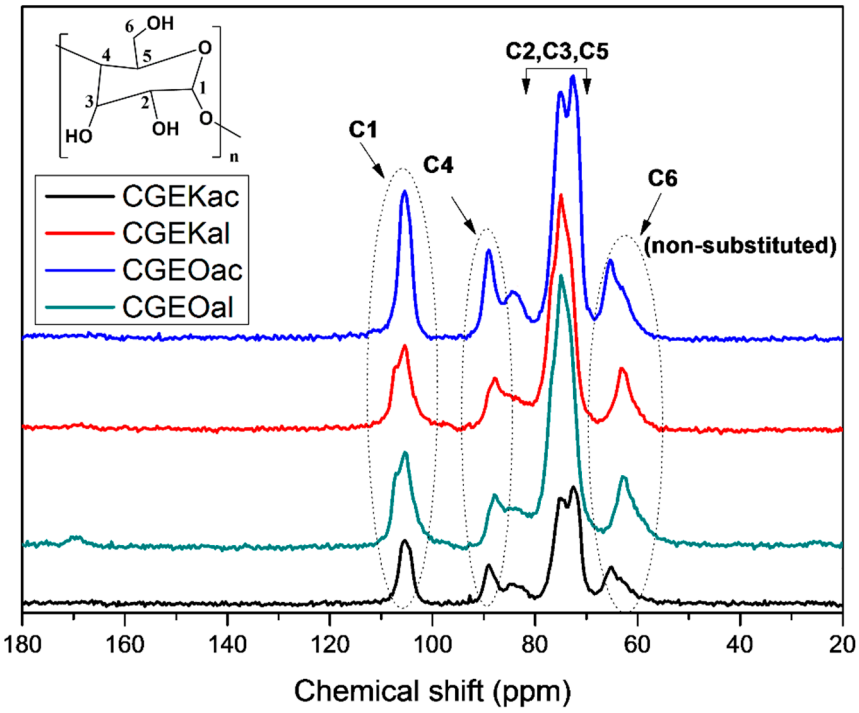


**Figure 2.** $^{13}C$ NMR spectra of the extracted cellulose samples using kraft and organosolv procedures followed by either acidified sodium chlorite or alkaline hydrogen peroxide treatment.

The sample's Crystallinity Index (*CrI*) can be calculated from the relationship between integration areas of ordered cellulose ($A_{86–92ppm}$) and amorphous cellulose ($A_{79–86ppm}$) at C4 signals using the Larsson formula [41,42] as follows:

$$CrI,\ \% = \frac{A_{86-92ppm}}{A_{86-92ppm} + A_{79-86ppm}} \times 100 \quad (1)$$

The *CrI* of samples were 59%, 55%, 50%, and 49% for CGEOac, CGEKac, CGEOal, and CGEKal, respectively. It is noticed that samples modified with acidified sodium chlorite

present enhanced crystallinity compared with alkaline-peroxide-treated samples. This observation consolidates well with the FTIR results.

### *3.4. Molecular Weight Distribution of the Samples*

Table 3 summarizes the molecular weight distributions of EG cellulosic samples. The polydispersity index ($PD_I$) was calculated as $M_w/M_n$, whereas the apparent number-average degree of polymerization ($DP_n$) and weight-average degree of polymerization ($DP_w$) were calculated by dividing respectively $M_n$ and $M_w$ values by 519, which corresponds to the monomer equivalent weight of CTC. To the best of our knowledge, there are no data in the literature dealing with the molecular weight distribution of EG cellulose.

**Table 3.** Parameters obtained from GPC analysis for cellulose samples.

| Sample | $M_w$ | $M_n$ | $PD_I$ | $DP_w$ | $DP_n$ |
|---|---|---|---|---|---|
| CGEKac | 381,218 | 26,976 | 14.13 | 735 | 52 |
| CGEkal | 400,856 | 81,436 | 4.92 | 772 | 156 |
| CGEOac | 470,845 | 32,370 | 14.54 | 907 | 62 |
| CGEOal | 495,308 | 98,339 | 5.04 | 954 | 189 |

Clearly, organosolv gave higher values of $M_n$ and $M_w$ than the kraft treatment, which is due to the harsh hydrolysis conditions of the kraft process, as reported in the chemical composition section. Nevertheless, the most important difference is observed between acidified chlorite and alkaline peroxide treatments. Those differences are probably related to the treatment chemicals and conditions. Indeed, $M_n$ and $M_w$ are obviously lower for samples treated with acidified chlorite. This decrease in molecular weight and polydispersity of cellulose samples suggests that degradation occurred during the process [43]. This phenomenon is caused by the depolymerization of cellulose by the cleavage of the glycosidic bond, which means that the adopted process generates smaller fragments of cellulose [23].

It is reported that according to the extraction method, cellulose polymer possesses an average degree of polymerization of 300–3000 and accordingly an average molecular weight of 50.000–500.000 g/mol [44]. Apparently, the obtained results correspond well to the literature, and the obtained results are similar to those reported for α-cellulose extracted from oil palm fronds [23] and esperato grass [30].

### *3.5. Morphological Analysis*

The morphological investigation was performed using SEM and all micrographs are depicted in Figure 3. Long and individual fibers are observed with smooth and clean surfaces. As demonstrated in previous characterizations, this is due to the removal of most non-cellulosic plant components by the employed treatment procedures. It can also be observed that cellulose samples subjected to acidified sodium chlorite treatment are fragmented, in contrast to those modified by alkaline peroxide solution. This observation corresponds well to the molecular weight distribution discussion, where the same samples exhibited lower molecular weight which is explained by the fragmentation of cellulose [23].

The extracted MCC samples have a modified irregular rod-like shape and a slightly rough surface, which is due to hydrochloric acid hydrolysis that caused cellulose fiber degradation [6,23]. It is worth mentioning that acid hydrolysis leads to the fragmentation of pyranose linkages, ensuring the deterioration of amorphous regions with a decrease in fiber lengths.

The dimensions of the fibers were calculated using Image J software. For MCC samples, diameters of about 11.7 ± 1.8 µm, 6.12 ± 2.9 µm, 7.39 ± 1.3 µm, and 6.38 ± 2.6 µm were reported for MCCGEKac, MCCGEKal, MCCGEOac, and MCCGEOal, respectively, whereas lengths of 61.6 ± 6.4 µm, 67.1 ± 7.2 µm, 56.9 ± 8.4 µm, and 60.3 ± 7.5 µm were found for MCCGEKac, MCCGEKal, MCCGEOac, and MCCGEOal samples, correspondingly.

These findings reflect the microscale of the obtained MCC, indicating the efficiency of the employed hydrolysis methods. Moreover, the obtained results are similar and comparable to those reported in the literature. Indeed, the reported lengths are similar to those of MCC extracted from Eucalyptus sulfate pulp [45] and Posidonia oceanica [46].

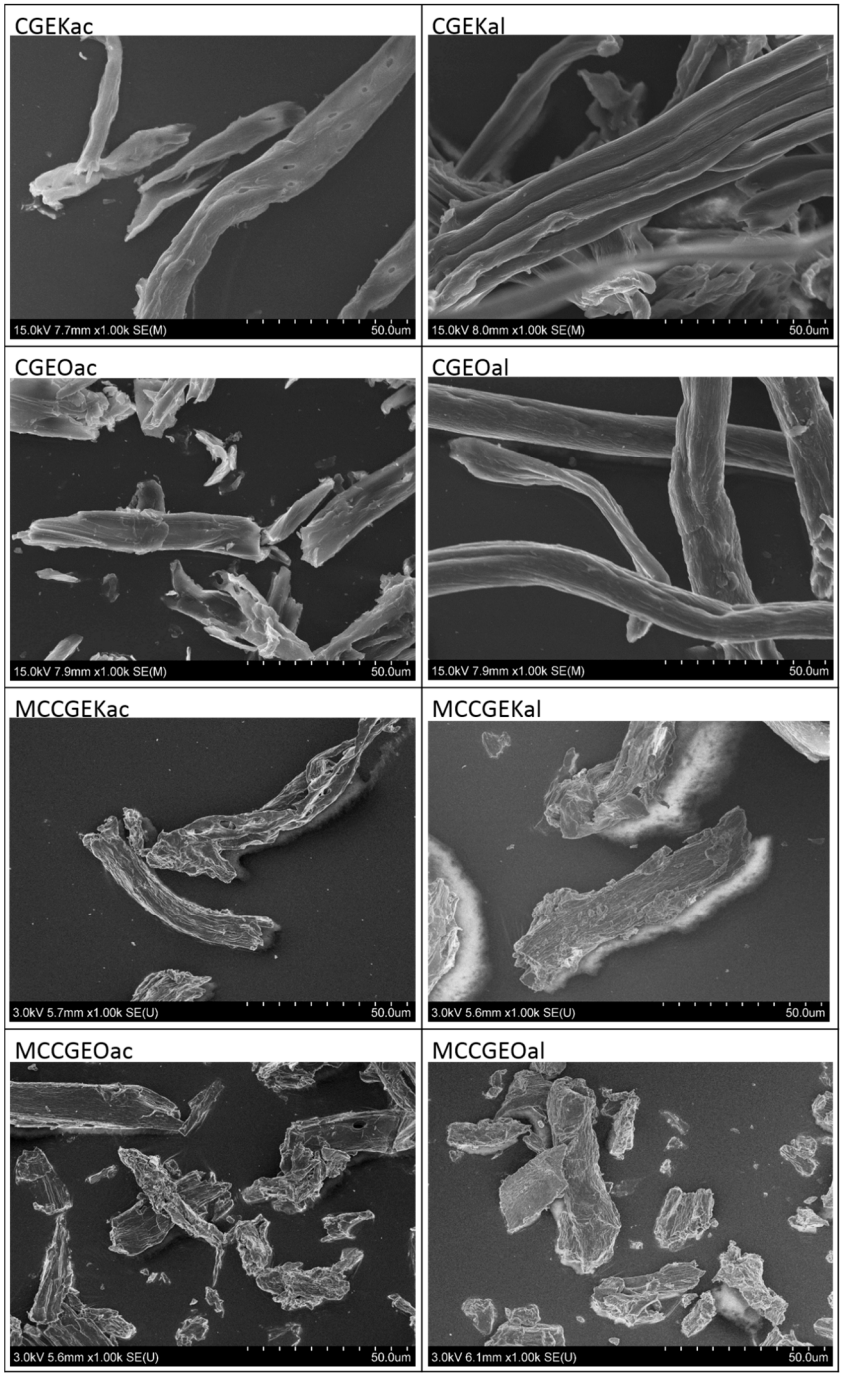


**Figure 3.** SEM images of extracted cellulose and MCC using kraft and organosolv procedures followed by either acidified sodium chlorite or alkaline hydrogen peroxide treatment.

### *3.6. Thermal Stability*

The thermal stability of cellulose and MCC samples was evaluated by DSC and TGA analyses. The exploration of this property is crucial for assessing the material performance for advanced applications. Materials with high thermal stability enable large and advanced applications. Indeed, some preparation processes, such as composites preparation, occur at

relatively high temperatures of around 200 °C [34], which make the identification of the degradation profile of the lignocellulosic materials more than necessary.

Figure 4 shows the obtained TGA thermograms, the derivative thermograms (DTG) are also exhibited in the same figure. Figure 5 displays the DSC curves of all samples. The reported data are described in Table 4.

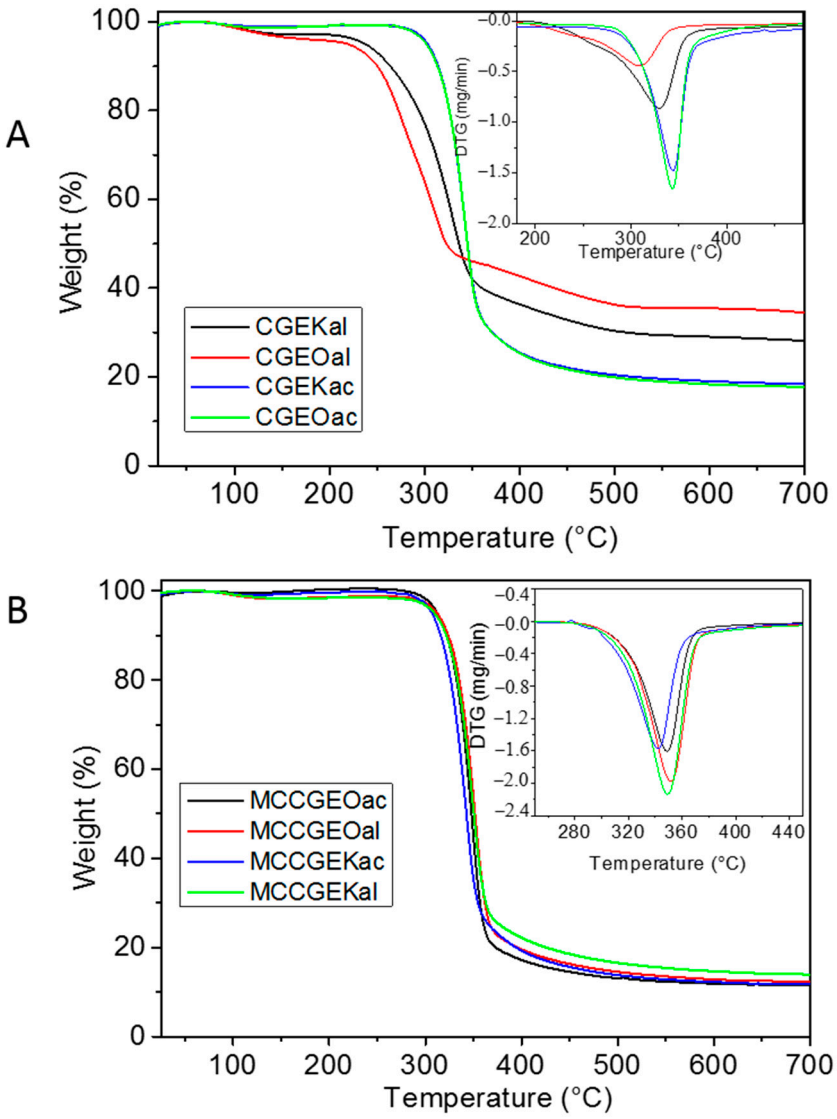


**Figure 4.** TGA thermograms of (**A**) cellulose and (**B**) MCC samples along with the corresponding DTG curves.

The TGA curves display two weight loss steps. The first occurring within the range of 50 to 160 °C with a mass loss of about 6% corresponds to surface-absorbed moisture evaporation. The second weight loss of about 80% is related to cellulose glycosyl unit degradation processes, comprising dehydration, decarboxylation, depolymerization, and decomposition, accompanied by char formation within the range of 250 to 420 °C.

Furthermore, in cellulose samples, it can be observed that alkaline-peroxide-treated samples display lower thermal stability. Three decomposition steps are noticed for which the degradation starts at lower temperatures. The first process is assigned to water evaporation, the two other steps are attributed to the cellulose with an earlier degradation that might be assigned to the amorphous parts [47,48]. Indeed, the thermal stability of cellulose depends strongly upon its crystallinity degree [49]. These observations are in good accordance with the reported results derived from FTIR analysis.

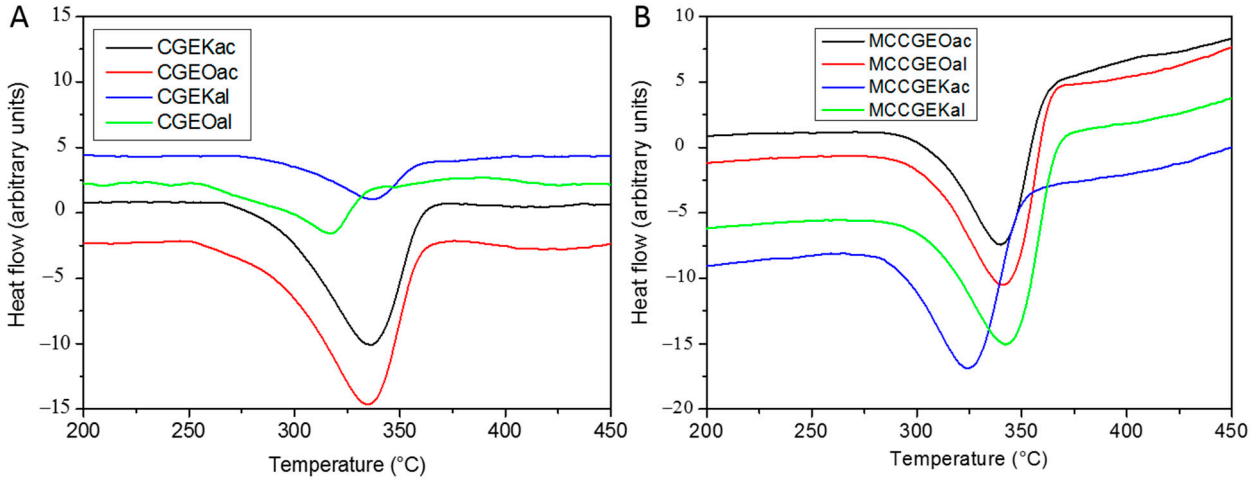


**Figure 5.** DSC curves of (**A**) extracted cellulose and (**B**) MCC samples using kraft and organosolv procedures followed by either acidified sodium chlorite or alkaline hydrogen peroxide treatment.

**Table 4.** TGA/DSC data for cellulose and MCC studied samples.

| Sample | TGA Analysis | | | DSC Analysis | | |
|---|---|---|---|---|---|---|
| | Onset (°C) [a] | Peak (°C) [b] | wt (%) [c] | $T_i$ (°C) [d] | $T_m$ (°C) [e] | ΔH (J/g) [f] |
| MCCGEOac | 318.9 | 348.8 | 82.8 | 307.5 | 345.1 | 383.1 |
| MCCGEOal | 322.3 | 351.6 | 80.4 | 314.3 | 350.8 | 360.6 |
| MCCGEKac | 307.3 | 342.2 | 80.6 | 298.8 | 336.1 | 399.3 |
| MCCGEKal | 317.9 | 349.2 | 77.8 | 302.7 | 342.8 | 379.9 |
| CGEOac | 308.8 | 343.3 | 74.6 | 289.8 | 335.3 | 374.7 |
| CGEOal | 272.7 | 311.1 | 57.2 | 282.2 | 317.1 | 297.1 |
| CGEKac | 296.4 | 342.9 | 74.4 | 291.4 | 335.6 | 377.9 |
| CGEKal | 268.6 | 329.2 | 63.6 | 300.2 | 335.9 | 270.1 |

[a] Onset decomposition temperature. [b] Peak temperature of DTGA. [c] Residual weight at 400 °C. [d] Onset decomposition temperature using DSC results. [e] Peak temperature using DSC results. [f] Heat of decomposition.

Better thermal stability is noticed for the extracted MCC samples, which is reflected by the increase in the decomposition temperatures compared with the cellulose samples. The samples display identical behavior independently from the cellulose extraction techniques. Indeed, thermal decomposition occurs at around 350 °C, which presents similar thermal stability as the commercial MCC [34], MCC extracted from Kenaf bast [50], MCC from oil palm empty fruit bunch [51], and MCC from date seeds (*Phoenix dactylifera* L.) [29]. Furthermore, a better thermal behavior is obtained for our MCC samples compared with MCC isolated from waste Leucaena leucocephala seeds [52] and sacred Bali bamboo [53]. These observations reflect the efficiency of the employed techniques and the high thermal stability of the MCC extracted from Eucalyptus Globulus.

DSC curves present one endothermic peak at around 320–350 °C, referring to cellulose 1,4 glycosidic bond cleavage resulting in cellulose volatilization to levoglucosan and char [30]. MCC samples show higher degradation temperatures compared with their native cellulose samples, reflecting the high crystallinity. The decomposition peaks are well resolved and narrower, in contrast to those of cellulose, confirming once again the elimination of hemicellulose and high purity [33]. Indeed, the high molecular ordering leads to high decomposition properties, thus to enhanced thermal stability [54].

## 4. Conclusions

As a summary of the paper findings, α-cellulose was successfully isolated from Eucalyptus Globulus through kraft or organosolv delignification followed by bleaching using

either acidified sodium chlorite or alkaline peroxide treatments. MCC samples were subsequently produced by acid hydrolysis. The exploited treatments demonstrated their efficiency in the elimination of the non-cellulosic matters, for which the purest MCC is achieved with the organosolv treatment followed by the acidic bleaching. A deep characterization was performed by FTIR, NMR, TGA/DSC, SEM, and GPC to determine the $\alpha$-cellulose and MCC compositions, structures, morphologies, and thermal stabilities. The obtained results indicated that the physicochemical features of the prepared MCC from EG are very satisfying and comparable to commercial MCC. Furthermore, this work revealed that EG-MCC produced from organosolv combined with acidic treatments provided relatively better characteristics with micro-sized structure, high purity, and good thermal features, rendering it a prominent candidate for a wide range of uses such as reinforced-polymer composites with enhanced thermal properties, dietary food, packaging, films, as well as smart and energetic materials.

**Author Contributions:** Conceptualization, D.T.; Methodology, W.B. and D.T.; Formal analysis, W.B., A.F.T. and A.A.; Investigation, D.T.; Data curation, W.B.; Writing—original draft, W.B. and A.A.; Writing—review & editing, D.T., A.F.T., M.H.H. and N.B. All authors have read and agreed to the published version of the manuscript.

**Funding:** This research received no external funding.

**Institutional Review Board Statement:** Not applicable.

**Informed Consent Statement:** Not applicable.

**Data Availability Statement:** The data presented in this study are available on request from the corresponding author.

**Conflicts of Interest:** The authors declare no conflict of interest.

## References

1. Saba, N.; Tahir, P.M.; Jawaid, M. A review on potentiality of nano filler/natural fiber filled polymer hybrid composites. *Polymers* **2014**, *6*, 2247–2273. [CrossRef]
2. Brongniart, A.; Pelouze, T.; Dumas, A. Rapport sur un mémoire de m. Payen, relatif à la composition de la matière ligneuse. *CR Hebd. Seances Acad. Sci.* **1839**, *8*, 51–53.
3. Jablonsky, M.; Majova, V.; Skulcova, A.; Haz, A. Delignification of pulp using deep eutectic solvents. *J. Hyg. Eng. Des.* **2018**, *22*, 76–81.
4. Majová, V.; Strizincová, P.; Jablonsky, M.; Skulcova, A.; Vrska, M.; Malvis Romero, A. Deep eutectic solvents: Delignification of wheat straw. In Proceedings of the World Sustain, Energy Days (WSED), Wels, Austria, 1–3 March 2017.
5. Majova, V.; Jablonsky, M.; Skulcova, A.; Ondrigova, K. Delignification of pulp with two ternary deep eutectic solvents: Urea-acetamide-glycerol and malic acid-proline-lactic acid. *J. Hyg. Eng. Des.* **2019**, *26*, 76–80.
6. Beroual, M.; Boumaza, L.; Mehelli, O.; Trache, D.; Tarchoun, A.F.; Khimeche, K. Physicochemical properties and thermal stability of microcrystalline cellulose isolated from esparto grass using different delignification approaches. *J. Polym. Environ.* **2021**, *29*, 130–142. [CrossRef]
7. Mamaye, M.; Kiflie, Z.; Feleke, S.; Yimam, A. Evaluation and optimization of kraft delignification and single stage hydrogen peroxide bleaching for ethiopian sugarcane bagasse. *J. Nat. Fibers* **2022**, *19*, 1226–1238. [CrossRef]
8. Shatalov, A.A.; Pereira, H. High-grade sulfur-free cellulose fibers by pre-hydrolysis and ethanol-alkali delignification of giant reed (*Arundo donax* L.) stems. *Ind. Crops Prod.* **2013**, *43*, 623–630. [CrossRef]
9. Silva, N.; Silva, N.; Mulinari, D. Influence of sequential acid-alkali treatment on palm biomass waste properties. *J. Nat. Fibers* **2021**, *19*, 7502–7516. [CrossRef]
10. Vaidya, A.A.; Murton, K.D.; Smith, D.A.; Dedual, G. A review on organosolv pretreatment of softwood with a focus on enzymatic hydrolysis of cellulose. *Biomass Convers. Biorefinery* **2022**, *12*, 5427–5442. [CrossRef]
11. Bijok, N.; Fiskari, J.; Gustafson, R.R.; Alopaeus, V. Modelling the kraft pulping process on a fibre scale by considering the intrinsic heterogeneous nature of the lignocellulosic feedstock. *Chem. Eng. J.* **2022**, *438*, 135548. [CrossRef]
12. Kleinert, T.; Tayenthal, K. Über neuere versuche zur trennung von cellulose und inkrusten verschiedener hölzer. *Angew. Chem.* **1931**, *44*, 788–791. [CrossRef]
13. Florian, T.D.M.; Villani, N.; Aguedo, M.; Jacquet, N.; Thomas, H.G.; Gerin, P.; Magali, D.; Richel, A. Chemical composition analysis and structural features of banana rachis lignin extracted by two organosolv methods. *Ind. Crops Prod.* **2019**, *132*, 269–274. [CrossRef]

14. Michelin, M.; Liebentritt, S.; Vicente, A.A.; Teixeira, J.A. Lignin from an integrated process consisting of liquid hot water and ethanol organosolv: Physicochemical and antioxidant properties. *Int. J. Biol. Macromol.* **2018**, *120*, 159–169. [CrossRef] [PubMed]
15. Axelsson, L.; Franzén, M.; Ostwald, M.; Berndes, G.; Lakshmi, G.; Ravindranath, N. Jatropha cultivation in southern india: Assessing farmers' experiences. *Biofuels Bioprod. Biorefining* **2012**, *6*, 246–256. [CrossRef]
16. Hernández-Hernández, H.; Chanona-Pérez, J.; Terrés, E.; Vega, A.; Ligero, P.; Farrera-Rebollo, R.; Villanueva, S. Microscopy and spectroscopy tools for the description of delignification. *Cellul. Chem. Technol* **2019**, *53*, 87–97. [CrossRef]
17. Zhao, X.; Cheng, K.; Liu, D. Organosolv pretreatment of lignocellulosic biomass for enzymatic hydrolysis. *Appl. Microbiol. Biotechnol.* **2009**, *82*, 815–827. [CrossRef] [PubMed]
18. Shatalov, A.A.; Pereira, H. Papermaking fibers from giant reed (*Arundo donax* L.) by advanced ecologically friendly pulping and bleaching technologies. *BioResources* **2006**, *1*, 45–61. [CrossRef]
19. Thakur, V.K. *Cellulose-Based Graft Copolymers: Structure and Chemistry*; CRC Press: Boca Raton, FL, USA, 2015.
20. Kleppe, P.J. Kraft pulping. *Tappi* **1970**, *53*, 35–47.
21. Santos, A.; Rodríguez, F.; Gilarranz, M.A.; Moreno, D.; García-Ochoa, F. Kinetic modeling of kraft delignification of eucalyptus globulus. *Ind. Eng. Chem. Res.* **1997**, *36*, 4114–4125. [CrossRef]
22. Esteves, C.V.; Sevastyanova, O.; Östlund, S.; Brännvall, E. Differences and similarities between kraft and oxygen delignification of softwood fibers: Effects on chemical and physical properties. *Cellulose* **2021**, *28*, 3149–3167. [CrossRef]
23. Trache, D.; Hussin, M.H.; Chuin, C.T.H.; Sabar, S.; Fazita, M.N.; Taiwo, O.F.; Hassan, T.; Haafiz, M.M. Microcrystalline cellulose: Isolation, characterization and bio-composites application—A review. *Int. J. Biol. Macromol.* **2016**, *93*, 789–804. [CrossRef] [PubMed]
24. Moreira, R.; Mendes, C.V.; Banaco, M.B.F.; Carvalho, M.G.V.; Portugal, A. New insights in the fractionation of pinus pinaster wood: Sequential autohydrolysis, soda ethanol organosolv and acidic precipitation. *Ind. Crops Prod.* **2020**, *152*, 112499. [CrossRef]
25. Tocco, D.; Carucci, C.; Monduzzi, M.; Salis, A.; Sanjust, E. Recent developments in the delignification and exploitation of grass lignocellulosic biomass. *ACS Sustain. Chem. Eng.* **2021**, *9*, 2412–2432. [CrossRef]
26. Pereira, P.H.F.; Ornaghi Jr, H.L.; Arantes, V.; Cioffi, M.O.H. Effect of chemical treatment of pineapple crown fiber in the production, chemical composition, crystalline structure, thermal stability and thermal degradation kinetic properties of cellulosic materials. *Carbohydr. Res.* **2021**, *499*, 108227. [CrossRef] [PubMed]
27. Poke, F.S.; Raymond, C.A. Predicting extractives, lignin, and cellulose contents using near infrared spectroscopy on solid wood in eucalyptus globulus. *J. Wood Chem. Technol.* **2006**, *26*, 187–199. [CrossRef]
28. Carrillo, I.; Mendonça, R.T.; Ago, M.; Rojas, O.J. Comparative study of cellulosic components isolated from different eucalyptus species. *Cellulose* **2018**, *25*, 1011–1029. [CrossRef]
29. Abu-Thabit, N.Y.; Judeh, A.A.; Hakeem, A.S.; Ul-Hamid, A.; Umar, Y.; Ahmad, A. Isolation and characterization of microcrystalline cellulose from date seeds (*Phoenix dactylifera* L.). *Int. J. Biol. Macromol.* **2020**, *155*, 730–739. [CrossRef]
30. Trache, D.; Donnot, A.; Khimeche, K.; Benelmir, R.; Brosse, N. Physico-chemical properties and thermal stability of microcrystalline cellulose isolated from alfa fibres. *Carbohydr. Polym.* **2014**, *104*, 223–230. [CrossRef]
31. Daraei Garmakhany, A.; Sheykhnazari, S. First principles of pretreatment and cracking biomass to fundamental building blocks. *Introd. Renew. Biomater. First Princ. Concepts* **2017**, 181–217. [CrossRef]
32. Fodil Cherif, M.; Trache, D.; Brosse, N.; Benaliouche, F.; Tarchoun, A.F. Comparison of the physicochemical properties and thermal stability of organosolv and kraft lignins from hardwood and softwood biomass for their potential valorization. *Waste Biomass Valorization* **2020**, *11*, 6541–6553. [CrossRef]
33. Kian, L.; Saba, N.; Jawaid, M.; Fouad, H. Characterization of microcrystalline cellulose extracted from olive fiber. *Int. J. Biol. Macromol.* **2020**, *156*, 347–353. [CrossRef] [PubMed]
34. Bessa, W.; Trache, D.; Derradji, M.; Bentoumia, B.; Tarchoun, A.F.; Hemmouche, L. Effect of silane modified microcrystalline cellulose on the curing kinetics, thermo-mechanical properties and thermal degradation of benzoxazine resin. *Int. J. Biol. Macromol.* **2021**, *180*, 194–202. [CrossRef] [PubMed]
35. El Achaby, M.; Kassab, Z.; Barakat, A.; Aboulkas, A. Alfa fibers as viable sustainable source for cellulose nanocrystals extraction: Application for improving the tensile properties of biopolymer nanocomposite films. *Ind. Crops Prod.* **2018**, *112*, 499–510. [CrossRef]
36. Ajouguim, S.; Abdelouahdi, K.; Waqif, M.; Stefanidou, M.; Saâdi, L. Modifications of alfa fibers by alkali and hydrothermal treatment. *Cellulose* **2019**, *26*, 1503–1516. [CrossRef]
37. Kalita, R.D.; Nath, Y.; Ochubiojo, M.E.; Buragohain, A.K. Extraction and characterization of microcrystalline cellulose from fodder grass; setaria glauca (l) p. Beauv, and its potential as a drug delivery vehicle for isoniazid, a first line antituberculosis drug. *Colloids Surf. B Biointerfaces* **2013**, *108*, 85–89. [CrossRef]
38. Tarchoun, A.F.; Trache, D.; Klapötke, T.M.; Krumm, B.; Mezroua, A.; Derradji, M.; Bessa, W. Design and characterization of new advanced energetic biopolymers based on surface functionalized cellulosic materials. *Cellulose* **2021**, *28*, 6107–6123. [CrossRef]
39. Wawer, I.; Witkowski, S. Analysis of solid state 13c nmr spectra of biologically active compounds. *Curr. Org. Chem.* **2001**, *5*, 987–999. [CrossRef]
40. Borchani, K.E.; Carrot, C.; Jaziri, M. Untreated and alkali treated fibers from alfa stem: Effect of alkali treatment on structural, morphological and thermal features. *Cellulose* **2015**, *22*, 1577–1589. [CrossRef]

41. Larsson, P.T.; Westermark, U.; Iversen, T. Determination of the cellulose iα allomorph content in a tunicate cellulose by cp/mas 13c-nmr spectroscopy. *Carbohydr. Res.* **1995**, *278*, 339–343. [CrossRef]
42. Liitiä, T.; Maunu, S.L.; Hortling, B. Solid state nmr studies on cellulose crystallinity in fines and bulk fibres separated from refined kraft pulp. *Holzforschung* **2000**, *54*, 618–624. [CrossRef]
43. Chen, J.H.; Guan, Y.; Wang, K.; Xu, F.; Sun, R.C. Regenerated cellulose fibers prepared from wheat straw with different solvents. *Macromol. Mater. Eng.* **2015**, *300*, 793–801. [CrossRef]
44. Trache, D. Microcrystalline cellulose and related polymer composites: Synthesis, characterization and properties. *Handb. Compos. Renew. Mater. Struct. Chem.* **2016**, *1*, 61–92.
45. Li, J.; Zhang, X.; Zhang, M.; Xiu, H.; He, H. Optimization of selective acid hydrolysis of cellulose for microcrystalline cellulose using fecl3. *BioResources* **2014**, *9*, 1334–1345. [CrossRef]
46. Trache, D.; Tarchoun, A.F.; De Vita, D.; Kennedy, J.F. *Posidonia oceanica* (L.) delile: A mediterranean seagrass with potential applications but regularly and erroneously referred to as an algal species. *Int. J. Biol. Macromol.* **2022**, *230*, 122624. [CrossRef] [PubMed]
47. Hachaichi, A.; Kouini, B.; Kian, L.K.; Asim, M.; Fouad, H.; Jawaid, M.; Sain, M. Nanocrystalline cellulose from microcrystalline cellulose of date palm fibers as a promising candidate for bio-nanocomposites: Isolation and characterization. *Materials* **2021**, *14*, 5313. [CrossRef] [PubMed]
48. Hideno, A. Comparison of the thermal degradation properties of crystalline and amorphous cellulose, as well as treated lignocellulosic biomass. *BioResources* **2016**, *11*, 6309–6319. [CrossRef]
49. Shaikh, H.M.; Anis, A.; Poulose, A.M.; Al-Zahrani, S.M.; Madhar, N.A.; Alhamidi, A.; Alam, M.A. Isolation and characterization of alpha and nanocrystalline cellulose from date palm (*Phoenix dactylifera* L.) trunk mesh. *Polymers* **2021**, *13*, 1893. [CrossRef]
50. Aprilia, N.S.; Davoudpour, Y.; Zulqarnain, W.; Khalil, H.A.; Hazwan, C.C.M.; Hossain, M.; Dungani, R.; Fizree, H.; Zaidon, A.; Haafiz, M.M. Physicochemical characterization of microcrystalline cellulose extracted from kenaf bast. *BioResources* **2016**, *11*, 3875–3889. [CrossRef]
51. Ismail, F.; Othman, N.E.A.; Wahab, N.A.; Hamid, F.A.; Aziz, A.A. Preparation of microcrystalline cellulose from oil palm empty fruit bunch fibre using steam-assisted acid hydrolysis. *J. Adv. Res. Fluid Mech. Therm. Sci.* **2021**, *81*, 88–98. [CrossRef]
52. Husin, M.; Li, A.R.; Ramli, N.; Romli, A.Z.; Hakimi, M.I.; Ilham, Z. Preparation and characterization of cellulose and microcrystalline cellulose isolated from waste leucaena leucocephala seeds. *Int. J. Adv. Appl. Sci.* **2017**, *4*, 51–58. [CrossRef]
53. Abdul Khalil, H.; Lai, T.K.; Tye, Y.Y.; Paridah, M.; Fazita, M.; Azniwati, A.; Dungani, R.; Rizal, S. Preparation and characterization of microcrystalline cellulose from sacred bali bamboo as reinforcing filler in seaweed-based composite film. *Fibers Polym.* **2018**, *19*, 423–434. [CrossRef]
54. Tarchoun, A.F.; Trache, D.; Klapötke, T.M.; Derradji, M.; Bessa, W. Ecofriendly isolation and characterization of microcrystalline cellulose from giant reed using various acidic media. *Cellulose* **2019**, *26*, 7635–7651. [CrossRef]